VOL. 10, NO. 9, MAY 2015 ISSN 1819-6608
ARPN Journal of Engineering and Applied Sciences
©2006-2015 Asian Research Publishing Network (ARPN). All rights reserved.

www.arpnjournals.com

SAR IMAGE CHANGE DETECTION USING GAUSSIAN MIXTURE MODEL WITH SPATIAL INFORMATION

C. Iswarya[1], R. Meena Prakash[1] and R. Shantha Selva Kumari[2]
[1]Department of Electronics and Communication Engineering, P. S. R. Engineering College, Sivakasi, India
[2]Department of Electronics and Communication Engineering, Mepco Schlenk Engineering College, Sivakasi, India
E-Mail: iswarya.ece27@gmail.com

ABSTRACT

A novel method for unsupervised change detection in multi-temporal satellite images using Gaussian mixture model (GMM) with spatial information is proposed. This approach is based on three steps. Firstly, the difference image between two Synthetic Aperture Radar (SAR) images of the same area taken at two different times is obtained using the standard log–ratio operator. Secondly, a preprocessing step of anisotropic diffusion is applied to the difference image. Thirdly, Gaussian Mixture Model is used for segmentation of the difference image in which the parameters are estimated using Expectation algorithm. The standard GMM considers each pixel as independent and hence the segmentation is sensitive to speckle noise present in the SAR images. To incorporate the spatial information in segmentation, anisotropic preprocessing is done and also the posterior probability computed in the M step is weighted with the mean filter. The proposed method is tested on four sets of multi-temporal images. The obtained results demonstrate the effectiveness of the method in obtaining higher change detection accuracies compared to the related methods.

Keywords: gaussian mixture model, SAR image change detection, expectation maximization.

1. INTRODUCTION

Change Detection [4, 10] is the method of analyzing two images taken at different times over the same geographical area and identifying the changes that have taken place between the two different acquisition times. Synthetic Aperture Radar (SAR) system offers a wide coverage area and it is insensitive to the weather and illumination conditions. Hence it finds vast applications in Remote Sensing. The drawback existing in SAR image is that it they contain speckle noise. This makes the change detection of SAR images more challenging than the other optical images.

Artificial Immune System with multi-objective optimization algorithm is proposed [1] for change detection. A dissimilarity measure for change detection based on divisive normalization image representation is proposed in [2]. A similarity measure based on Kullback-Leibler divergence is proposed [3] in which the local statistics are modeled using GMM. An unsupervised change detection technique using GMM, local gradual descent and k-means clustering is proposed in [5]. A method [6] in which the difference image is modeled using GMM and Genetic Algorithm to estimate the parameters is proposed. An unsupervised change detection method based on Dual-Tree Complex Wavelet Transform (DT-CWT) is proposed [7]. A method in which the difference image is decomposed using undecimated discrete wavelet transform and the multiscale feature vectors are clustered using k-means algorithm is proposed [8]. Principal Component Analysis and k-means clustering are employed for change detection [9]. Thresholding of the difference image based on Kittler-Illingworth (KI) threshold selection criterion is proposed in [11]. Wavelet based multiscale decomposition of the difference image is proposed for change detection [12, 20]. Methods based on Markov Random Field and support vectors are also in research focus for change detection [13, 14, 15].

Gaussian Mixture Model is one of the prevalent methods for change detection in SAR images. But GMM is sensitive to noise since it does not consider the spatial dependencies. Anisotropic filter is one of the best tools for detail preserving smoothing [16, 17, 18]. Hence, in the proposed method, first the difference image between the two SAR images acquired at different times over the same geographical region is computed by using the log ratio operator or mean operator. Next, anisotropic filter used for preprocessing the difference image. The GMM is used for segmenting the difference image into changed pixels region and unchanged pixels region. The Expectation Maximization algorithm is used to estimate the model parameters in which the Maximization step is modified to incorporate the spatial information. The proposed method is tested on four different sets of SAR images and the efficiency is compared with the standard GMM and other methods in the literature.

2. GAUSSIAN MIXTURE MODEL AND EM

The Gaussian also known as the normal distribution of a single variable x, can be written in the form

$$N(x|\mu,\sigma^2) = \frac{1}{(2\pi\sigma^2)^{\frac{1}{2}}}\exp\left\{-\frac{1}{2\sigma^2}(x-\mu)^2\right\} \quad (1)$$

where μ is the mean and σ^2 is the variance.

The Expectation Maximization algorithm for Gaussian Mixtures is an iterative algorithm that starts from some initial estimate (e.g., random) and then proceeds iteratively until the value is detected. The EM algorithm consists of the following steps.

©2006-2015 Asian Research Publishing Network (ARPN). All rights reserved.

Step-1: Initialize the parameters - Means μ_k, covariances Σ_k and mixing coefficients π_k, and evaluate the initial value of the log likelihood.
Step-2: E step: Evaluate the responsibilities using the current parameter values.

$$\gamma(z_{nk}) = \frac{\pi_k N(x_n|\mu_k,\Sigma_k)}{\sum_{j=1}^{K}\pi_j N(x_n|\mu_j,\Sigma_j)} \quad (2)$$

Step-3: M step. Re-estimate the parameters described by the current responsibilities values

$$\mu_k^{new} = \frac{1}{N_k}\sum_{n=1}^{N}\gamma(z_{nk})x_n \quad (3)$$

$$\Sigma_k^{new} = \frac{1}{N_k}\sum_{n=1}^{N}\gamma(z_{nk})(x_n-\mu_k^{new})(x_n-\mu_k^{new})^T \quad (4)$$

$$\pi_k^{new} = \frac{N_k}{N} \quad (5)$$

$$N_k = \sum_{n=1}^{N}\gamma(z_{nk}) \quad (6)$$

Step-4: Evaluate the log likelihood value

$$\ln p(X|\mu,\Sigma,\pi) = \sum_{n=1}^{N}\ln\{\sum_{k=1}^{K}\pi_k N(x_n|\mu_k,\Sigma_k)\} \quad (7)$$

Check for convergence of either the parameter values or the log likelihood. When the convergence criterion is not satisfied, then go to step-2.

I. Anisotropic diffusion filter

The continuous anisotropic diffusion is given

$$\frac{\partial I_t(x,y)}{\partial t} = div[c_t \cdot \nabla I_t(x,y)] \quad (8)$$

Let $I_t(x,y)$ be the gray level at coordinates (x,y) of a digital image at iteration t, and $I_0(x,y)$ the original input image. The continuous anisotropic diffusion in Equation (8) can be discretely implemented by using four nearest neighbors and the Laplacian operator:

$$I_{t+1}(x,y) = I_t(x,y) + \frac{1}{\eta}\sum_{i=1}^{4}[c_t^i(x,y)\cdot\nabla I_t^i(x,y)] \quad (9)$$

where $\nabla I_t^i(x,y), i = 1,2,3,4$ represent the gradients of four neighbors in the north, south, east and west irections, respectively.

$$\begin{aligned}\nabla I_t^1(x,y) &= I_t(x,y-1) - I_t(x,y)\\ \nabla I_t^2(x,y) &= I_t(x,y+1) - I_t(x,y)\\ \nabla I_t^3(x,y) &= I_t(x+1,y) - I_t(x,y)\\ \nabla I_t^4(x,y) &= I_t(x-1,y) - I_t(x,y)\end{aligned} \quad (10)$$

$c_t^i(x,y)$ is the diffusion coefficient associated with $\nabla I_t^i(x,y)$ and is considered as a function of the gradient $c_t^i(x,y) = g(\nabla I_t^i(x,y))$. The diffusion coefficient function is given by

$$g(\nabla I) = 1/\left[1+\left(\frac{|\Delta I|}{k}\right)^2\right] \quad (11)$$

where k is a constant and must be fine tuned for the requirement. The anisotropic diffusion filter provides edge preserving smoothing and is applied as preprocessing for the difference image.

3. PROPOSED METHOD

The proposed method can be explained in the following steps.
Step-1: Two SAR images taken at two different times over the same geographical region are taken as inputs.
Step-2: The difference image is found out as given in Equations (12) or (13).
Step-3: Perform Anisotropic diffusion of the difference image using Equations (9) - (11).
Step-4: Assign the number of classes as 4 and initialize the mean, variance and the mixing coefficient for EM segmentation.
Step-5: Perform the Expectation Step using Equation (2) and estimate the posterior probability.
Step-6: Assign weights to the posterior probability using mean filter to incorporate the spatial information.
Step-7: Re-estimate the parameters – mean, variance and mixing coefficient using Equations (3) - (6).
Step-8: Evaluate the log likelihood and check for convergence.(<0.01)
Step-9: If the convergence criterion is not satisfied, go to step 5.
Step-10: Using the obtained final model, segmentation is done
Step-11: Label the unchanged pixels as value 0 for classes 1 to 3 and the changed pixels as value 255 for the class 4.

A. Image differencing method

The performance of the SAR image segmentation depends on the quality of the difference image. Difference image can be produced using the subtraction operator and the ratio operator
Ratio methods give better results for change detection. The two ratio methods are log ratio and mean ratio and in the proposed method both of them are used depending upon the quality of the difference image
obtained.

$$Difference\ Image = 1 - \min\left(\frac{\mu_1}{\mu_2},\frac{\mu_2}{\mu_1}\right) \quad (12)$$

where μ_1 and μ_2 represent the local mean values of the two input images.

©2006-2015 Asian Research Publishing Network (ARPN). All rights reserved.

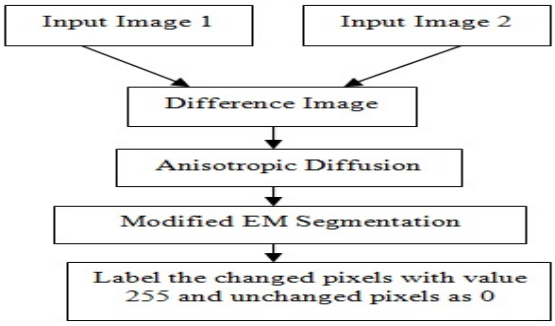

Figure-1. Block diagram of the proposed method.

B. Description of the data set

The proposed method is tested on four sets of data. The input images of the first dataset are JERS SAR channel 1 images of the airport at Cooinda, Kakadu National Park, Australia [20]. The second dataset input images are referenced in [20]. The third dataset consists of synthetic images modified in a region of interest and added with speckle noise. The fourth dataset consists of ESA Envisat ASAR image acquired in 12 April 2007 and 26 July 2007 collected on Bangladesh and parts of India [6].

C. Quantitative measures

- False Positive (FP) number: It is defined as unchanged pixels wrongly judged as changed pixels.
- False Negative (FN) number: It is defined as changed pixels that missed detection.
- Overall error (OE) number: The sum of FP and FN

$$OE=FP+FN \quad (13)$$

- Detection error in percentage

$$(PE) = OE/N \times 100 \quad (14)$$

where N is the total number of pixels.

D. Results and analysis

Figure-2, 3, 4 and 5 represent the results of the change detection experiments on the four datasets. (a) and (b) represent the input images taken at two different times, (c) represents the difference image, (d) represents the ground truth image, (e) represents the result of the standard GMM method and (f) represents the result of the proposed method.

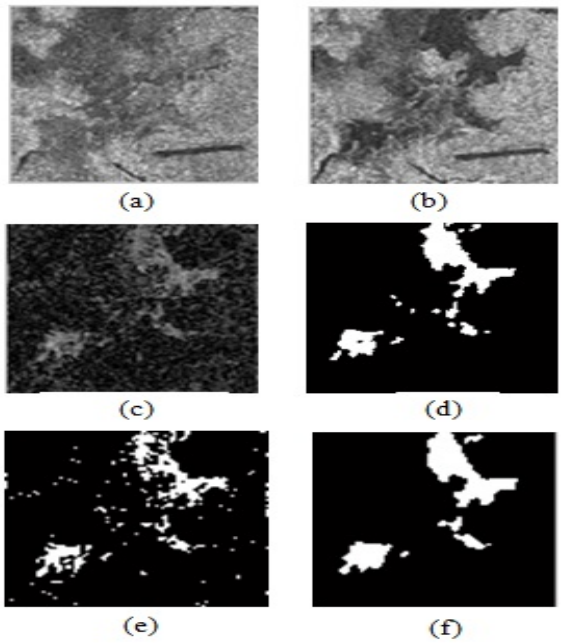

Figure-2. (a) &(b) input images, (c) Difference image, (d) Ground truth,(e) Standard GMM method (f) Proposed method.

The simulation results of FP, FN and PE by the standard GMM, proposed method and reference method for the four datasets are shown in Tables 1, 2, 3 and 4.

Table-1. Simulation Results on the first data set (Figure-2)

Methods	FP	FN	N	PE
Method [20]	927	1144	43,264	4.79
Standard GMM	1527	1662	43,264	7.37
Proposed method	1210	689	43,264	4.38

©2006-2015 Asian Research Publishing Network (ARPN). All rights reserved.

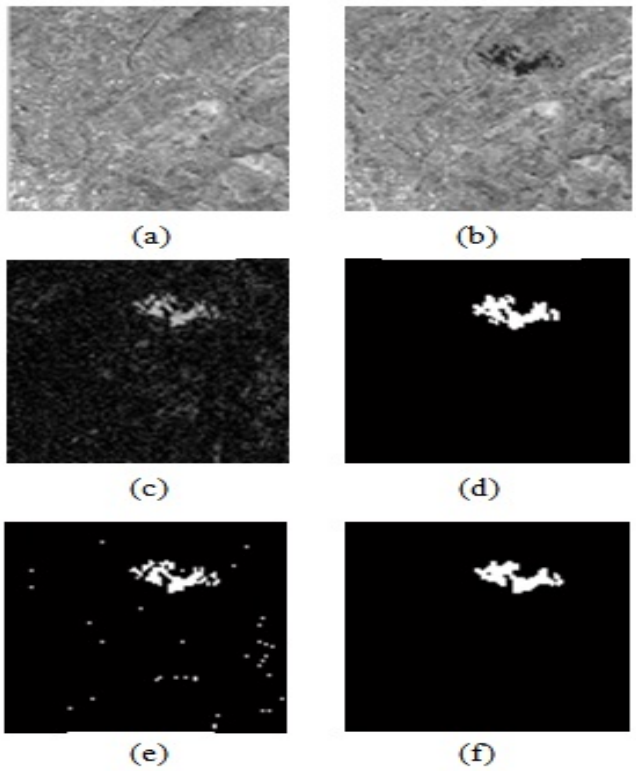

Figure-3. (a) &(b) input images, (c) Difference image, (d) Ground truth,(e) Standard GMM method, (f) Proposed method.

Table-2. Simulation results on the second dataset (Figure-3).

Methods	FP	FN	N	PE
Method [20]	278	242	1,02,400	0.50
Standard GMM	521	714	1,02,400	1.21
Proposed method	227	277	1,02,400	0.49

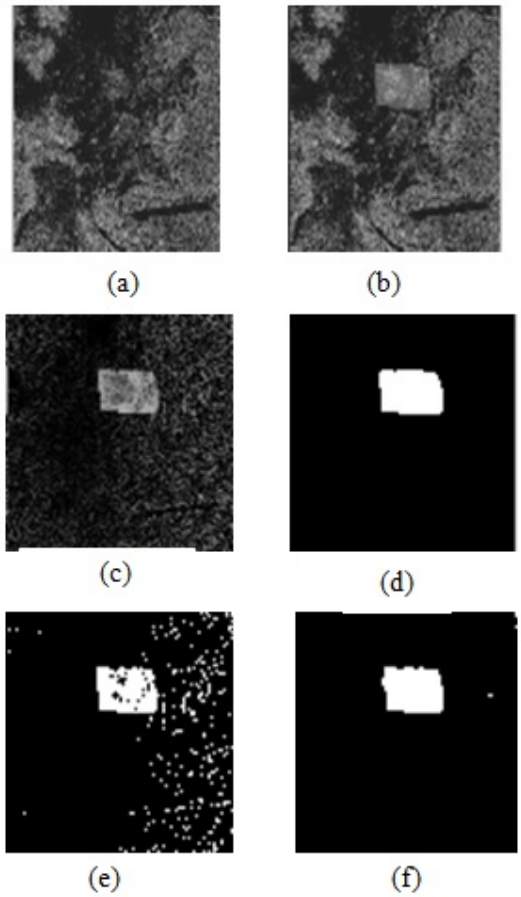

Figure-4. (a) & (b) input images, (c) Difference image, (d) Ground truth,(e) Standard GMM method (f) Proposed method.

Table-3. Simulation results on the third dataset (Figure-4).

Methods	FP	FN	N	PE
Method [20]	828	1289	1,02,400	2.07
Standard GMM	3712	649	1,02,400	4.26
Proposed method	230	218	1,02,400	0.44

©2006-2015 Asian Research Publishing Network (ARPN). All rights reserved.

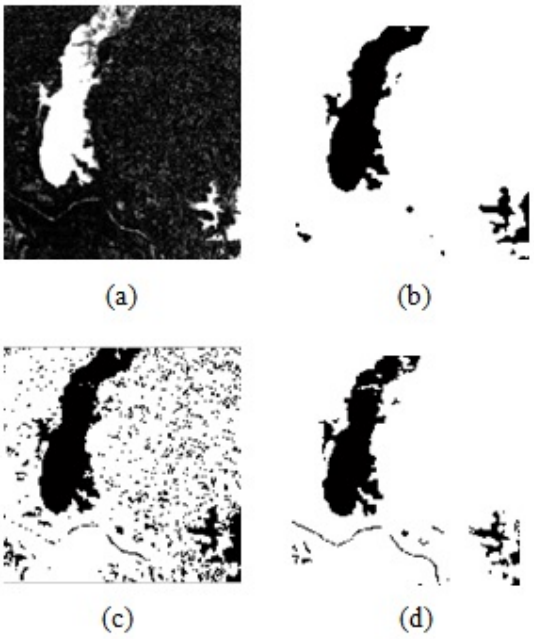

Figure-5. (a) Difference image, (b) Ground truth, (c) Standard GMM method, (d) Proposed method.

Table-4. Simulation results on the fourth dataset (Figure-5).

Methods	FP	FN	N	PE
Multiresolution Based Method [9]	158	4205	82,944	5.27
Standard GMM	1084	8766	82,944	11.88
Proposed method	1326	2261	82,944	4.32

From the change detection results obtained on the various datasets, it is inferred that the proposed method gives better segmentation accuracy of the changed pixels when compared to the other methods in literature both qualitatively and quantitatively.

4. CONCLUSIONS

A novel method for unsupervised change detection in multi-temporal satellite images using Gaussian mixture model with spatial information is proposed in this paper. The drawback of GMM based segmentation is that it is sensitive to noise. To overcome this, the spatial information is incorporated in segmentation by two techniques, one is through anisotropic preprocessing and the other is through the posterior probability in the Maximization Step of the Expectation Maximization algorithm. The proposed method has been tested on three sets of real SAR image and one set of synthetic SAR image. Results obtained show the efficiency of the method when compared to the other methods. The method is robust to speckle noise which is common in SAR images.

REFERENCES

[1] Ronghua Shang, Liping Qi, Licheng Jiao, Rustam Stolkin and Yangyang Li. 2014. "Change detection in SAR images by artificial immune multi-objective clustering", Pattern Recognit. Lett. Vol. 31, pp. 53–67, February.

[2] Qian Xu and Lina J. Karam. 2014. "Change Detection On SAR Images Using Divisive Normalization Based Image Representation", in: IEEE International Conference on Acoustic, Speech and Signal Processing, pp. 4372-4376, 2014.

[3] Qian Xu and Lina J. Karam. 2013. "Change Detection On SAR Images By A Parametric Estimation Of The KL-Divergence Between Gaussian Mixture Models", in: IEEE International Conference on Acoustic, Speech and Signal Processing, pp. 2109-2113.

[4] Masroor Hussain, Dongmei Chen, Angela Cheng, Hui Wei and David Stanley. 2013. "Change detection from remotely sensed images: From pixel-based to object-based approaches", ISPRS Journal of Photogrammetry and Remote Sensing. Vol. 80, pp. 91–106, April.

[5] Zeki Yetgin. 2012. "Unsupervised Change Detection of Satellite Images Using Local Gradual Descent," IEEE Transactions on Geoscience and Remote Sensing. Vol. 50, No.5, pp.1919–1929, May.

[6] Celik T. 2010. "Image change detection using Gaussian mixture model and genetic algorithm," J. Vis. Commun. Image Represent, Vol.21, pp. 965–974, September.

[7] T. Celik and K.-K. Ma. 2010. "Unsupervised change detection for satellite images using dual-tree complex wavelet transform," IEEE Transactions on Geoscience and Remote Sensing, Vol. 48, No.3, pp.1199–1210, March.

[8] Celik T. 2009. "Multiscale Change Detection in Multitemporal Satellite Images," IEEE Transactions on Geoscience and Remote Sensing, Vol.6, No.4, pp. 820–824, October.

[9] Celik T. 2009. "Unsupervised Change Detection in Satellite Images Using Principal Component Analysis and k-Means Clustering," IEEE

©2006-2015 Asian Research Publishing Network (ARPN). All rights reserved.

Transactions on Geoscience and Remote Sensing, Vol. 6, No.4, pp. 772–776, October.

[10] M. Torma, P. Harma and E. Jarvenpaa. 2007. "Change detection using spatial data problems and challenges," in IEEE International Geoscience and Remote Sensing Symposium, pp. 1947–1950.

[11] Yakoub Bazi, Lorenzo Bruzzone and Farid Melgani. 2005. "An Unsupervised Approach Based on the Generalized Gaussian Model to Automatic Change Detection in Multitemporal SAR Images," IEEE Transactions on Geoscience and Remote Sensing. Vol. 43, No.4, pp. 874– 887, April.

[12] Francesca Bovolo and Lorenzo Bruzzone. 2005. "A Detail-Preserving Scale-Driven Approach to Change Detection in Multitemporal SAR Images", IEEE Transactions on Geoscience and Remote Sensing, Vol. 43, No.12, pp. 2963– 2972, December.

[13] T. Kasetkasem and P. Varshney. 2002. "An image change detection algorithm based on markov random field models," IEEE Transactions on Geoscience and Remote Sensing , Vol. 40, No. 8, pp. 1815–1823, August.

[14] L. Bruzzone and D. Prieto. 2000. "Automatic analysis of the difference image for unsupervised change detection," IEEE Transactions on Geoscience and Remote Sensing, Vol. 38, No.3, pp. 1171–1182, May.

[15] L. Bruzzone and D. Prieto. 2000. "Automatic analysis of the difference image for unsupervised change detection," IEEE Transactions on Geoscience and Remote Sensing, Vol. 38, No.3, pp. 1171–1182, May.

[16] Sung In Cho, Suk-Ju Kang, Hi-Seok Kim and Young Hwan Kim. 2014. "Dictionary-based anisotropic diffusion for noise reduction", Pattern Recognit. Lett. Vol. 46, pp. 36–45, May.

[17] Shin-Min Chao and Du-Ming Tsai. 20103. "An improved anisotropic diffusion model for detail- and edge-preserving smoothing", Pattern Recognit. Lett. Vol. 31, pp. 2012–2023, June.

[18] Gui Gao, Lingjun Zhao, Jun Zhang, Diefei Zhou and Jijun Huang. 2008. "A segmentation algorithm for SAR images based on the anisotropic heat diffusion equation", Pattern Recognit. Lett. Vol. 41, pp. 3035–3043, January.

[19] C. M. Bishop. 2006. "Pattern Recognition and Machine Learning" New York: Springer.

[20] Dempster A.P., Laird N.M. and Rubin, D.B. 1977. "Maximum Likelihood from Incomplete Data via the EM Algorithm", Journal of the Royal Statistical Society, Vol. 39, No. 1, pp. 1-38.